Microscale simulations of the seismic response of flexible retaining walls

Simulations à l'échelle microscopique de la réponse sismique des murs de soutènement flexibles

Usama El Shamy & Saman Farzi Sizkow
Department of Civil and Environmental Engineering, Southern Methodist University, USA; e-mail: uelshamy@lyle.smu.edu

ABSTRACT: In this study, an analysis of soil-retaining wall dynamic interaction is conducted using three-dimensional Discrete Element Method (DEM) simulations. Soil grains are treated as rigid spherical particles that are allowed to overlap one another at contact points. The flexible sheetpile-type retaining wall is simulated using rigid balls glued together by parallel bonds. Free-field boundaries are employed at the lateral sides of the model to prevent the reflections of the propagating waves back to the assembly and enforce the free-field motion. Seismic excitation is introduced to the system through the base wall, which represents the bedrock. It is found that the lateral earth pressure and bending moment increase during seismic excitation and the final residual values are, in most cases, considerably larger than the initial static ones. It is also observed that the amount of wall deformation and the maximum level of internal forces and moments the sheetpile experiences during dynamic loading are strongly affected by the frequency of the input motion.

RÉSUMÉ : Dans cette étude, une analyse de l'interaction dynamique sol-mur de soutènement est menée à l'aide de simulations tridimensionnelles de la méthode des éléments discrets (DEM). Les grains du sol sont traités comme des particules sphériques rigides qui peuvent se chevaucher aux points de contact. Le mur de soutènement flexible de type palplanche est simulé à l'aide de billes rigides collées entre elles par des liaisons parallèles. Des limites de champ libre sont utilisées sur les côtés latéraux du modèle pour empêcher les réflexions des ondes se propageant vers l'ensemble et imposer le mouvement en champ libre. L'excitation sismique est introduite dans le système à travers la paroi de base, qui représente le substratum rocheux. On constate que la pression latérale de la terre et le moment de flexion augmentent pendant l'excitation sismique et les valeurs résiduelles finales sont, dans la plupart des cas, considérablement plus importantes que les valeurs statiques initiales. On observe également que la quantité de déformation de la paroi et le niveau maximal des forces et moments internes que la palplanche subit pendant le chargement dynamique sont fortement affectés par la fréquence du mouvement d'entrée.

KEYWORDS: Discrete element method, sheetpile, seismic loading, free-field boundaries

1 INTRODUCTION

Earthquakes can inflict serious damages on retaining walls including tilting and/or sliding of the wall. In addition, these wall movements can cause severe damages to the neighboring structures. There have been many reports documenting damages to retaining walls during earthquakes (Grivas and Souflis 1984, Pitilakis and Moutsakis 1989, Collin 1992, Tateyama et al. 1995, Tatsuoka et al. 1996, Fang et al. 2003, Huang and Chen 2004, Trandafir et al. 2009). The main factors responsible for these damages are the increase of lateral earth pressure on the wall, possible phase shift between wall and backfill motions and the accumulated tilt of the wall and its effect on the lateral earth pressure. Unfortunately, only few case histories investigating the behavior of retaining walls under seismic loading are properly documented. Therefore, numerical analysis and theoretical approaches play key roles in understanding the dynamic response of retaining walls. However, studying the dynamic response of soil-retaining wall systems is a very challenging task. Some of the main factors contributing to the complexity of the model are: soil non-linear behavior that affects its stiffness, geometric variation and its effect on the fundamental frequencies of the deposit, soil inhomogeneity in the form of the spatial variation in properties, dynamic soil-wall interaction as well as the dynamic characteristics of the wall.

The discrete element method is a very powerful numerical technique for modeling discontinuous media such as soil and is gaining increasing popularity among geotechnical engineers. This method has several advantages over other numerical techniques. The nonlinear soil behavior is inherently accounted for by the particles motion and their rearrangement. That in turn leads to creation and loss of some inter-particle contacts and possibly, sliding of particles. In addition, the spatial variation in properties of the deposit is guaranteed by the random generation of particles. DEM has been used by various researchers to study different phenomena regarding retaining walls. Chang and Chao (1994) used the discrete element method to investigate the active and passive earth pressure distribution developed during different modes of wall movement. Nadukuru and Michalowski (2012) conducted DEM simulations to obtain earth pressure distribution on retaining walls considering the arching effect and computed the centroid of stress distribution for the transitional and rotational wall movements. The plane-strain failure of dry-stone retaining walls was analyzed through two-dimensional DEM simulations by Oetomo et al. (2016) and the results were compared to the experimental data. Nadukuru and Michalowski (2012) examined the impact of dry granular flow in an inclined chute on a rigid wall. Non-spherical particles were used in the DEM simulations and the effect of inclination angle was also investigated. The previously mentioned studies are good examples showcasing discrete element method capability to handle problems pertaining to retaining structures. However, the dynamic response of soil-retaining wall systems which requires more complicated problem setup and more sophisticated dynamic boundary conditions was not in the scope of these studies.

In this paper, a microscale model is presented to simulate the dynamic response of sheetplie/granular backfill system using DEM. The soil deposit is modeled as an assembly of spherical, rigid particles which can interact with each other through contact

points. The sheetpile wall is created using small particles glued together by parallel bonds. The seismic load is introduced to the model by the base wall that represents the bedrock. Free-field boundaries are installed at both ends to avoid reflection of propagating waves into the assembly and apply the free-field motion. More details could be found in Sizkow and El Shamy (2021).

2 MODEL DESCRIPTION

The proposed approach was employed to investigate the response of a three degrees of freedom flexible wall retaining a dry granular backfill. In this study a gravitational field of 50 g is used, and scaling laws are applied to obtain the model dimensions. Periodic boundaries were installed at the front and back sides of the model to simulate an infinitely repeated system in the lateral direction and to avoid the reflection of propagating waves. The free-field boundary condition was implemented by a user-written code for the lateral sides of the deposit. This type of boundaries was employed to absorb the propagating waves and apply the free-field motion.

The heights of the soil deposit in front and behind the retaining wall were, respectively, 12 cm and 18 cm (6 m and 9 m in prototype units). The location of the right and left end boundaries were selected far enough (40 cm behind the wall and 14 cm in front of the wall in model units) to allow for full development of the failure wedges behind and in front of the wall. The soil deposit has a thickness of 3 cm (1.5 m in prototype units) and average porosity of 0.4. Soil particles constituting the deposit are of the size between 1.5 mm to 2.5 mm and have a density of 2650 kg/m^3. The properties of the backfill are presented in Table 1.

The flexible retaining wall had a free height of 6 cm (3 m in prototype units). The friction angle of the dry soil deposit was about 31 degrees. Note that the relatively small friction angle is mainly due to the employed spherical particles and almost uniform grain size distribution. Higher friction angles could be obtained by adopting particles of irregular shape (See Sizkow and El Shamy, 2021). The total calculated length of the wall was 13.5 cm (6.75 m in prototype units) and the sheetpile was assumed to be precast concrete panels and assigned an assumed thickness of 5 mm (25 cm in prototype units). The sheetpile was modeled by two sheets of particles with a size of 2.5 mm (total thickness of 5 mm). These particles were glued together using parallel bonds which can transmit both force and moment. The density of the concrete retaining wall was assumed to be 2400 kg/m^3, which resulted in each particle composing the wall to have a density of 4000 kg/m^3. The stiffness of the bonds was determined in a way that the modeled wall mimics the behavior of a concrete sheetpile with Young's modulus of 40 GPa. Other types of sheetpile walls such as steel sheetpiles could be modelled by using a different configuration of bonded particles and parallel bond properties. Figure 1 shows the final DEM model of the sheetpile/soil deposit system.

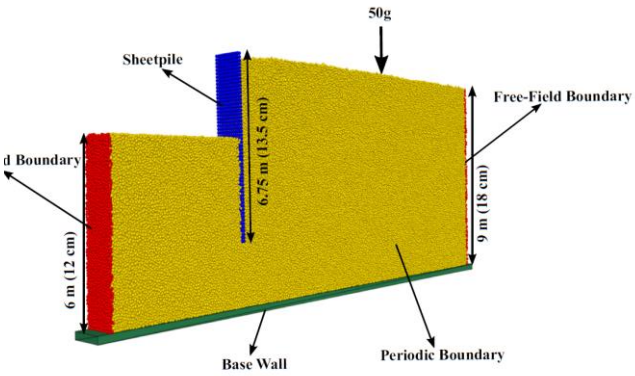

Figure 1. Granular deposit and retaining wall structure as modeled in DEM simulations

3 SIMULATION RESULTS

The sheetpile/backfill system was subjected to seismic base excitations with a maximum amplitude of 0.1g and frequencies of between 1 Hz to 6 Hz. The amplitude of the input motion gradually increased to reach its maximum value (0.1g) during the first 3 seconds, then it remained constant for the following 4 seconds, and it gradually vanished during the last second. The results obtained from these simulations are discussed.

Table 1. Backfill properties in prototype units

Dry unit weight	16 kN/m^3
Porosity	0.4
Void ratio	0.67
Angle of internal friction	31°
Fundamental frequency	5.8 Hz
Low strain shear wave velocity	210 m/s
Low strain shear modulus	70 MPa

Horizontal displacements of the sheetpile particles at different elevations were monitored during the DEM simulations, and the final position of the sheetpile was obtained. Figure 2 shows the deformed shape of the wall. It is evident from this figure that the displacements of the sheetpile are mostly rigid rotations, and the pivot point is located near the bottom of the wall. In addition, the results show that the maximum wall displacement corresponds to the input motion with the frequencies of 4 Hz and 5 Hz.

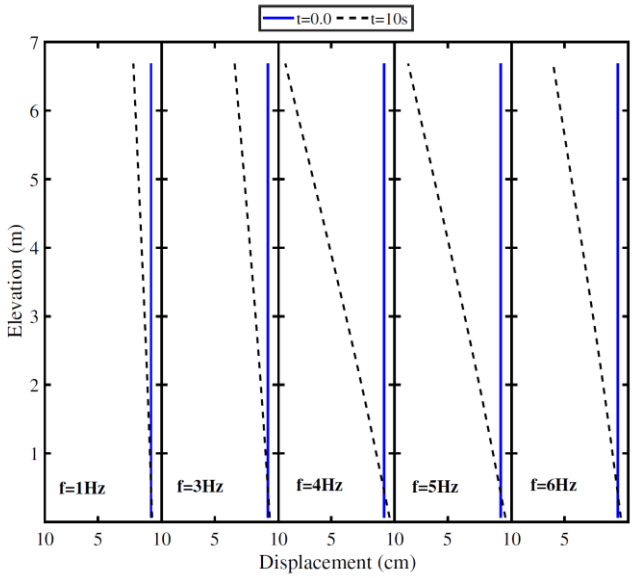

Figure 2. Sheetpile deformed shape

Figure 3 shows the initial static, maximum dynamic, and residual lateral earth pressure distributions on both sides of the sheetpile. The results show that the lateral earth pressure on the excavated side substantially increases during dynamic loading, especially for the input motion frequencies of 4 Hz to 6 Hz that have similar maximum dynamic and residual earth pressures. However, for the input motion frequencies of 1 Hz and 3 Hz, the maximum dynamic and residual passive earth pressures are significantly smaller.

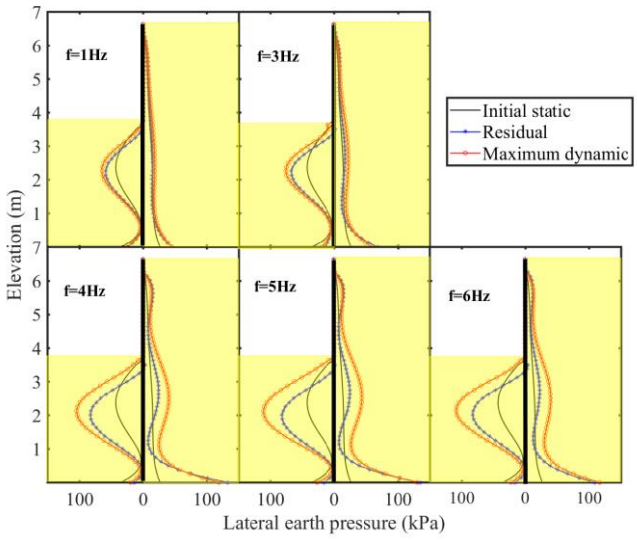

Figure 3. Lateral earth pressure distribution along both sides of the sheetpile

To further study the increase in the passive earth pressure on the excavated side of the sheetpile, the coefficient of earth pressure at a point located at 1.5 m below the dredge level in front of the wall was monitored during the simulations. Figure 4 shows the dynamic and average coefficients of earth pressure at this point versus wall rotation for input motion frequencies of 3 Hz to 6 Hz. It can be observed that during simulations with input frequencies of 4 Hz, 5 Hz and 6 Hz, the wall experienced enough rotation to activate the full passive strength of the soil down to 1.5 m below the dredge line on the excavated side. However, input motion frequencies of 1 Hz and 3 Hz do not produce enough wall rotation to mobilize the full passive strength at this point.

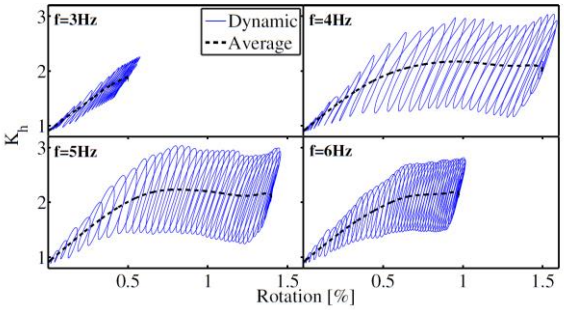

Figure 4. Coefficient of earth pressure versus wall rotation

Figure 5 shows the total soil thrust on both sides of the sheetpile. It can be seen that the total active soil thrust behind the sheetpile increases during dynamic loading due to the acceleration of the retained soil. It is also observed that the total passive and active soil thrusts in front and behind the sheetpile remain equal and in opposite directions during the simulations.

Figure 6 shows the initial static, maximum dynamic, and residual bending moments over the length of the sheetpile. It is observed that, for all cases, both maximum dynamic and residual bending moments are significantly higher than the initial static moment. This was expected because of the higher dynamic and residual lateral earth pressure on the sheetpile.

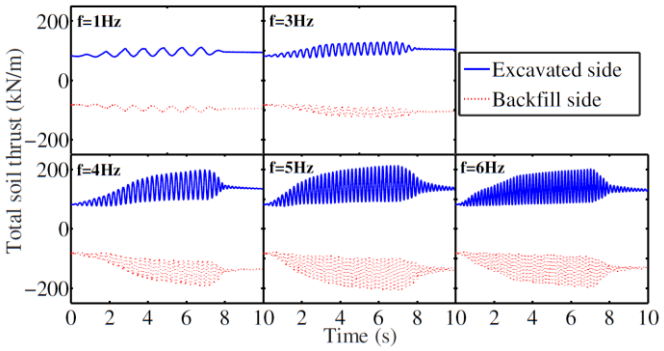

Figure 5. Time histories of total soil thrust

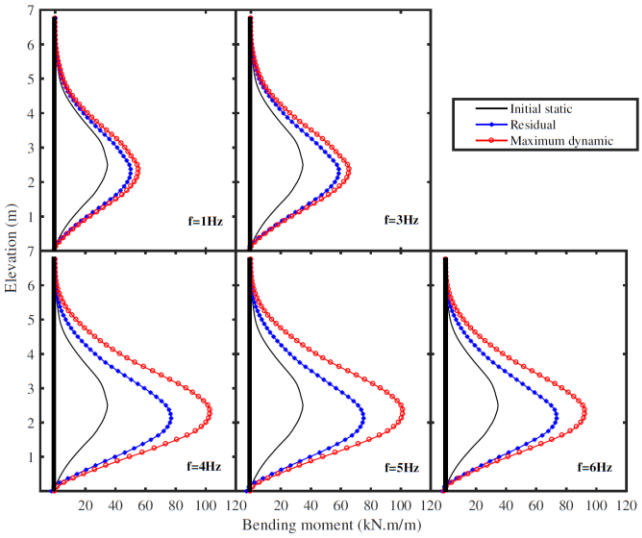

Figure 6. Bending moment profiles along the sheetpile

Figure 7 shows the development of maximum shear strain inside the soil deposit. In order to obtain the maximum shear strain at every location, strain tensors were tracked during the simulation within spherical volumes throughout the soil deposit. Eigenvalues of the shear strain tensors were calculated and time-histories for maximum shear strain at every location were determined.

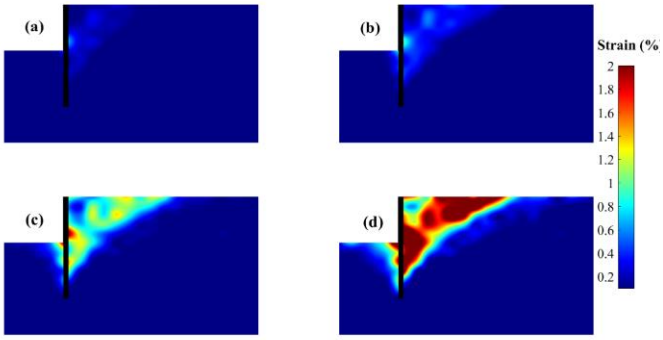

Figure 7. Shear strain at different time instances during the 0.1g-5Hz simulation: a) 1.5 s, b) 2.0 s, c) 3.5 s, and d) 9.0 s.

Investigation of changes in maximum shear strain throughout the deposit revealed that a failure surface was formed during the simulation. In Figure 7, the strain magnitude is demonstrated by different colors for the 0.1 g-5 Hz simulation. The wedges clearly resemble a Coulomb-like planar failure surface.

Figure 8 shows the ground settlement for different frequencies. It is obvious that most of the ground settlement has occurred near the sheetpile and there is almost no settlement at distances more than 8 m from the sheetpile. The largest ground settlement corresponds to an input motion with a frequency of 5 Hz.

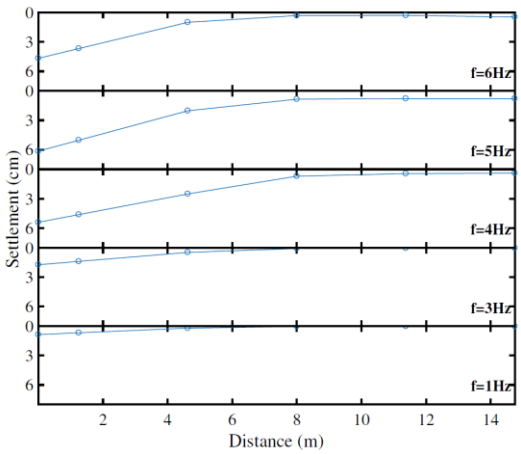

Figure 8. Ground settlement versus distance from the sheetpile

4 CONCLUSIONS

A DEM microscale approach is presented to evaluate the seismic response of a cantilever retaining wall/backfill system in the time-domain. The presented approach accounts for several factors such as: nonlinear behavior of the soil, dynamic soil-retaining wall interaction, sliding and rotation of the sheetpile, possible separation between sheetpile and backfill motions and dynamic characteristics of the flexible retaining wall. Pressure distributions on the sides of the wall change with the wall rotation and as the wall tilts the full strength of the soil in a larger region of the soil on the excavated side becomes mobilized. The results show that the maximum dynamic and residual passive lateral earth pressures and bending moments on the sheetpile are considerably higher than the initial static values. Failure wedges are formed in front and behind the sheetpile during the seismic loading and become larger as the simulation progresses. This is accompanied with ground settlement in the backfill especially near the sheetpile. In addition, it was found that the amount of deformation the wall experiences and the maximum level of its internal forces and moments during dynamic loading are strongly affected by the frequency of the input motion.

The obtained results highlight the strength of the proposed DEM-based approach and its ability to model large-scale boundary value problems. The simulations took on average around 30 hours on a 36-core processor to finish. The trends observed in this study were similar to published experimental and analytical results. One of the biggest advantages of this method is its seamless nature in the sense that the input parameters can be physically interpreted and do not change with the change of the simulated deposit and wall.

5 ACKNOWLEDGEMENTS

This research was partially supported by the US Army Corps of Engineers Engineer Research and Development Center, grant number W9132V-13-C-0004 and the National Science Foundation award number CMMI-1728612. These supports are gratefully acknowledged.

6 REFERENCES

Chang C.S. and Chao S.J. 1994. Discrete element analysis for active and passive pressure distribution on retaining wall. *Computers and Geotechnics*, 16(4), 291–310.

Collin J. 1992. Field observation of reinforced soil structures under seismic loading. *Proc. Of Earth Reinforcement Practice*, 223–228.

Fang Y., Yang Y., and Chen T. 2003. Retaining walls damaged in the chi-chi earthquake. *Canadian Geotechnical Journal*, 40(6), 1142–1153.

Grivas D. and Souflis C. 1984. Performance of the plateas wingwall during the 1981 earthquakes in Greece. *Proc. of the 8th World Conf. on Earthquake Engineering.* Oakland, Vol. 3, 509–515.

Huang C.C. and Chen Y.H. 2004. Seismic stability of soil retaining walls situated on slope. *Journal of Geotechnical and Geoenvironmental Engineering*, 130(1), 45–57.

Nadukuru S.S. and Michalowski R.L. 2012. Arching in distribution of active load on retaining walls. *Journal of Geotechnical and Geoenvironmental Engineering*, 138(5), 575–584.

Oetomo J.J., Vincens E., Dedecker F., and Morel J.C. 2016. Modeling the 2d behavior of dry stone retaining walls by a fully discrete element method. *International Journal for Numerical and Analytical Methods in Geomechanics*, 40(7), 1099–1120.

Pitilakis K. and Moutsakis A. 1989. Seismic analysis and behaviour of gravity retaining walls: The case of kalamata harbour quaywall. *Soils and Foundations*, 29(1), 1–17.

Sizkow, S.F, and El Shamy, U. 2021. Discrete element method simulations of the seismic response of flexible retaining walls," *Journal of Geotechnical and Geoenvironmental Engineering*, ASCE, 147(2), 04020157.

Sizkow, S.F, and El Shamy, U. 2021. SPH-DEM Simulations of Saturated Granular Soils Liquefaction Incorporating Particles of Irregular Shape, *Computers and Geotechnics*, 134, 104060

Tateyama M., Tatsuoka F., Koseki J., and Horii K. 1995. Damage to soil retaining walls for railway embankments during the great Hanshin-Awaji earthquake, January 17, 1995. *Earthquake Geotechnical Engineering.*

Tatsuoka F., Tateyama M., and Koseki J. 1996. Performance of soil retaining walls for railway embankments. *Soils and Foundations, 36(Special)*, 311–324.

Trandafir A.C., Kamai T., and Sidle R.C. 2009. Earthquake-induced displacements of gravity retaining walls and anchor-reinforced slopes. *Soil Dynamics and Earthquake Engineering*, 29(3), 428–437.